THE JOURNAL OF COMPARATIVE NEUROLOGY 493:274–290 (2005)

Immunohistochemical Localization of GAD67-Expressing Neurons and Processes in the Rat Brainstem: Subregional Distribution in the Nucleus Tractus Solitarius

ANGELINA Y. FONG,[1,2] RUTH L. STORNETTA,[3] C. MICHAEL FOLEY,[2,4] AND JEFFREY T. POTTS[1,2,4]*

[1]Department of Physiology, Wayne State University School of Medicine, Detroit, Michigan 48201

[2]Dalton Cardiovascular Research Center, University of Missouri-Columbia, Columbia, Missouri 65211

[3]Department of Pharmacology, University of Virginia, Charlottesville, Virginia 22908

[4]Department of Biomedical Sciences, University of Missouri-Columbia, Columbia, Missouri 65211

ABSTRACT

The role of γ-aminobutyric acid (GABA) in homeostatic control in the brainstem, in particular, in the nucleus tractus solitarius (NTS), is well established. However, to date, there is no detailed description of the distribution of GABAergic neurons within the NTS. The goal of the current study was to reexamine the efficacy of immunohistochemical localization of glutamic acid decarboxylase (GAD) protein, specifically the 67-kDa isoform (GAD67), as a marker for GABAergic neurons in the medulla and to provide a detailed map of GAD67-immunoreactive (-ir) cells within rat NTS by using a recently developed mouse monoclonal antibody. We describe a distribution of GAD67-ir cells in the medulla similar to that reported previously from in situ hybridization study. GAD67-ir cells were localized in regions known to contain high GABA content, including the ventrolateral medulla, raphe nuclei, and area postrema, but were absent from all motor nuclei, although dense terminal labeling was discerned in these regions. In the NTS, GAD67-ir was localized in all subregions. Semiquantitative analysis of the GAD67-ir distribution in the NTS revealed greater numbers of GAD67-ir cells medial to the solitary tract. Finally, dense GAD67 terminal labeling was found in the medial, central, intermediate, commissural, and subpostremal subregions, whereas sparse labeling was observed in the ventral subregion. Our findings support the use of immunohistochemistry for GAD67 as a marker for the localization of GABAergic cells and terminal processes in the rat brainstem. Furthermore, the reported heterogeneous distribution of GAD67-ir in the NTS suggests differential inhibitory modulation of sensory processing. J. Comp. Neurol. 493:274–290, 2005.

Indexing terms: GABA; medulla; sensory processing; inhibitory neurotransmitter

Grant sponsor: National Institutes of Health; Grant number: HL059167 (to J.T.P., A.Y.F.); Grant number: HL28785 (to R.L.S.); Grant sponsor: Children's Research Centre of Michigan (to J.T.P., A.Y.F.); Grant sponsor: Children's Hospital of Michigan; Grant number: CRCM-440017 (to J.T.P., A.Y.F.); Grant sponsor: National Aeronautics and Space Administration; Grant number: NNA04CC62G (to C.M.F.).

*Correspondence to: Jeffrey T. Potts, Dalton Cardiovascular Research Center, University of Missouri-Columbia, 134 Research Park Drive, Columbia, MO 65211. E-mail: pottsjt@missouri.edu

Received 28 January 2005; Revised 10 June 2005; Accepted 7 July 2005

DOI 10.1002/cne.20758

Published online in Wiley InterScience (www.interscience.wiley.com).

The amino acid γ-aminobutyric acid (GABA) is the major inhibitory neurotransmitter in the mammalian central nervous system (CNS). GABA in the CNS is ubiquitous and has been implicated in a wide range of functions and disease states, including neurological disorders, such as mood disorder, anxiety, and schizophrenia (for review see Brambilla et al., 2003; Wong et al., 2003), and autonomic functions, including cardiovascular (Ruggiero et al., 1985; Sved and Sved, 1990), respiratory (Tabata et al., 2001; Kuwana et al., 2003), and gustatory control (Bradley et al., 1996; Leonard et al., 1999).

GABA is synthesized from the amino acid glutamate by the enzyme glutamic acid decarboxylase (GAD). Two isoforms of GAD have been identified with molecular weights of 65,000 and 67,000 (Erlander et al., 1991), referred to as GAD65 and GAD67, respectively. Immunohistochemical (IHC) localization of GAD (Blessing et al., 1984; Meeley et al., 1985; Esclapez et al., 1994; Ellenberger, 1999) and, more recently, in situ hybridization (ISH) to the mRNA for the GAD isoforms (Esclapez et al., 1994; Chan and Sawchenko, 1998; Stornetta and Guyenet, 1999; Tanaka et al., 2003) have been utilized as markers of GABAergic neurons. In combination, these studies have demonstrated a widespread distribution of GAD-containing neurons throughout the rat neuroaxis (Esclapez et al., 1994), including a number of regions of the brainstem involved in autonomic regulation, such as the ventrolateral medulla (VLM; Chan and Sawchenko, 1998; Ellenberger, 1999; Stornetta and Guyenet, 1999; Tanaka et al., 2003) and the nucleus tractus solitarius (NTS; Blessing et al., 1984; Meeley et al., 1985; Chan and Sawchenko, 1998; Ellenberger, 1999; Stornetta and Guyenet, 1999; Tanaka et al., 2003).

The NTS, located within the dorsomedial medulla oblongata, is the site of integration of peripheral afferent input to the central nervous system, receiving primary afferents from cardiovascular, respiratory, gastrointestinal, and gustatory receptors (Kumada et al., 1990; Van Giersbergen et al., 1992; Dampney, 1994; Lawrence and Jarrott, 1996). In the rat, the NTS extends from the caudal border of the pons through to the spinomedullary junction. The cytoarchitecture of the NTS is highly complex and consists of a heterogeneous distribution of cells, which is further subdivided into a number of subregions (Kumada et al., 1990; Van Giersbergen et al., 1992). GABAergic neurotransmission within the NTS is well known to be involved in cardiovascular regulation (Kubo and Kihara, 1987, 1988; Miura et al., 1996), control of respiration (Tabata et al., 2001), and gustatory functions (Bradley et al., 1996).

Although the presence of both GABA (Dietrich et al., 1982; Maley and Newton, 1985; Izzo et al., 1992) and GAD (Blessing et al., 1984; Meeley et al., 1985; Chan and Sawchenko, 1998; Ellenberger, 1999; Stornetta and Guyenet, 1999; Tanaka et al., 2003) has been demonstrated within the NTS of both cats and rats, respectively, no systematic description of the regional distribution of GAD67 protein throughout the rostrocaudal axis of the rat NTS has been reported to date. Although the study by Esclapez and colleagues (1994) provided a detailed description of IHC labeling of GAD67 in the rat forebrain and midbrain, their observations did not extend to the medulla. Furthermore, in previous IHC studies, it was unclear which isoform of GAD was studied (Blessing et al., 1984; Meeley et al., 1985; Ellenberger, 1999; Liu et al., 2001, 2002). Moreover, to date, the polyclonal antibodies provide predominantly terminal labeling (Liu et al., 2001, 2002) and require pretreatment with the microtubule-interfering agent colchicine to enhance cell body labeling (Blessing et al., 1984; Ruggiero et al., 1985; Meeley et al., 1985; Ellenberger, 1999). Finally, the reported distribution of GAD-expressing cells in the NTS differs between ISH and IHC localization studies. ISH studies demonstrated dense labeling of GAD mRNA expressing cells in the NTS (Stornetta and Guyenet, 1999; Tanaka et al., 2003), but previous IHC studies demonstrated a lower density of GAD-expressing cells (Blessing et al., 1984; Meeley et al., 1985; Ellenberger, 1999). Similarly, studies utilizing antibodies to GABA, which often required different fixation methods (Maley and Newton, 1985; Izzo et al., 1992), have also demonstrated a much lower concentration of GABAergic neurons. In the present study, we re-examined the distribution of the GAD67 protein, as a marker for GABAergic neurons, throughout the adult rat medulla by using a recently developed mouse monoclonal antibody that allowed visualization of both GAD67-containing somata and terminal processes without colchicine pretreatment. Moreover, owing to the documented role of GABAergic inhibition on autonomic regulation, we sought to provide a detailed description of subregional distribution of GAD67 immunoreactivity within the NTS.

MATERIALS AND METHODS

Experiments were performed in accordance with the regulations stipulated in the U.S. Department of Health and Human Services and were approved by the Animal Investigation Committee at Wayne State University School of Medicine.

Tissue preparation

Adult, male Sprague-Dawley rats (n = 4, 280–320 g; Harlan) were deeply anesthetized with a mixture of ketamine (60 mg) and xylazine (8 mg, i.p.) and transcardially perfused with 100 ml 0.1 M PBS (pH 7.4), followed by 400–500 ml 4% paraformaldehyde in PBS (0.1 M, pH 7.4). The brains were removed and postfixed in the same fixative overnight at 4°C. Coronal sections (50 μm) of the medulla were collected on a vibratome (Vibratome 1000, St. Louis, MO) in 0.1 M PBS between bregma levels –12.42 mm to –14.53 mm. The sections were transferred into and stored in 0.1 M PBS (pH 7.4) at 4°C. Every fourth section collected was counterstained (0.5% neutral red; Sigma, St. Louis, MO), and the remaining sections were processed for immunohistochemistry within 48 hours of sectioning.

IHC of GAD67 in medulla

The IHC procedure used in the present study was modified and adapted from procedures described previously (Fong et al., 2002). All incubations in the IHC procedure were performed at room temperature, and all washes were performed in 0.1 M PBS (pH 7.4). Free-floating sections were incubated in 0.3% hydrogen peroxide for 30 minutes to quench endogenous peroxidase before incubation in a preblocking solution (30 minutes) of 10% normal goat serum (NGS; Vector, Burlingame, CA) in 0.1 M PBS, then rinsed briefly prior to 48 hours of incubation in monoclonal mouse anti-GAD67 antiserum (1:1,000; MAB5406; Chemicon, Temecula, CA) with 3% NGS in 0.1 M PBS (pH 7.4). No permeabilizing agent was utilized, because prelimi-

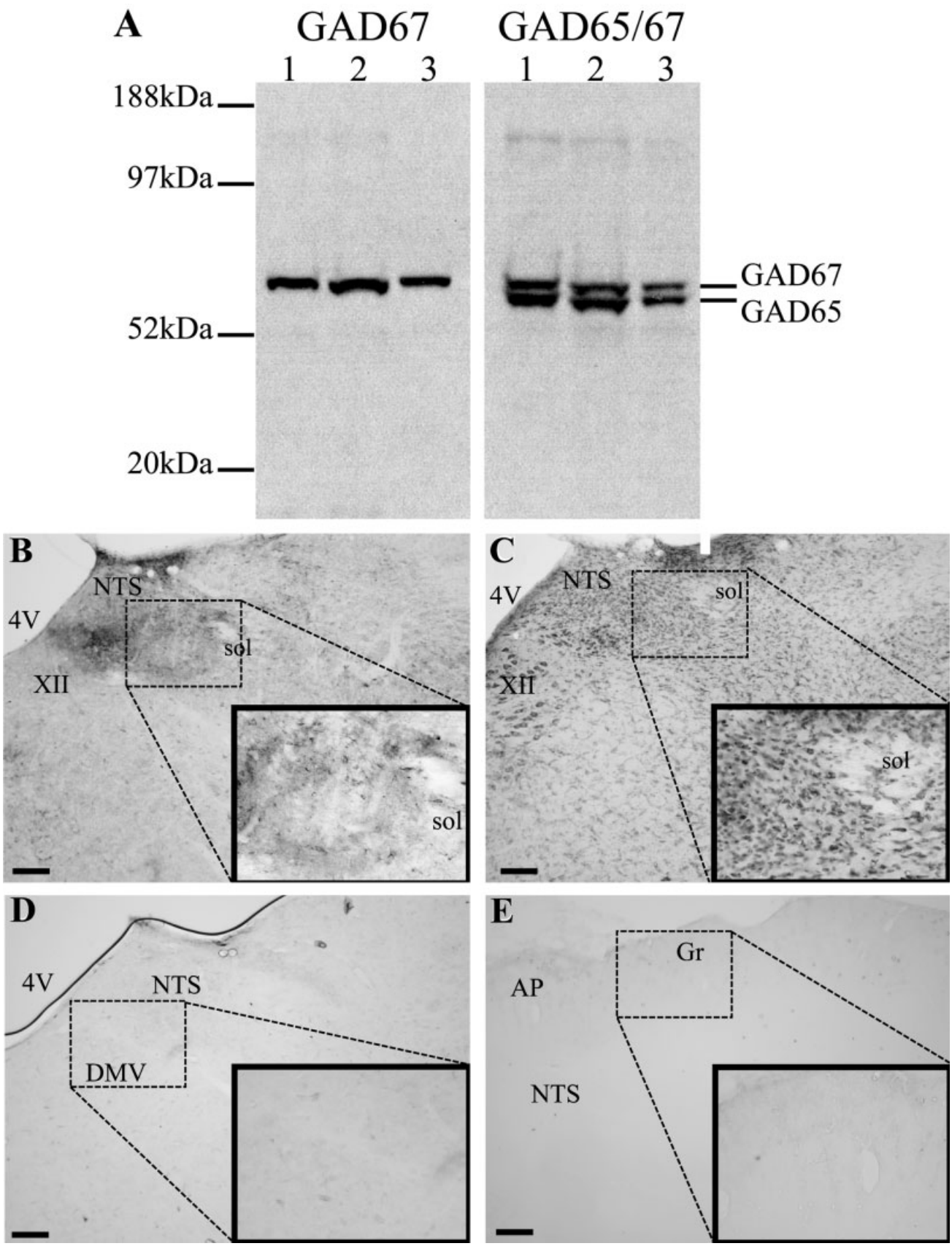
A
GAD67
GAD65/67
1 2 3
1 2 3
188kDa
97kDa
52kDa
20kDa
GAD67
GAD65
B
NTS
4V
sol
XII
sol
C
4V
NTS
sol
XII
sol
D
4V
NTS
DMV
E
Gr
AP
NTS

Figure 1

nary studies demonstrated that the presence of permeablizing agents, such as Triton X-100, or cryosectioning reduced labeling of cell bodies. At the end of the incubation in primary antiserum, the sections were thoroughly washed, then incubated for 2 hours in goat anti-mouse biotinylated IgG (1:200; Vector) with 3% NGS in 0.1 M PBS (pH 7.4). The sections were again washed and incubated in ABC Elite kit (Vector) for 1 hour. After further washes, the sections were exposed to nickel-enhanced diaminobenzidine (0.02% DAB, 0.2% $NiSO_4$) for 10 minutes prior to the addition of hydrogen peroxide (0.000015% final concentration), with the reaction terminated when it was deemed completed via observation under a dissecting microscope (approximately 6–8 minutes). The sections were transferred into fresh PBS (0.1 M, pH 7.4) before being mounted onto glass microscope slides in 0.5% gelatin, air dried, dehydrated in increasing concentrations of alcohol, cleared with xylene, and coverslipped with DPX (Sigma). Additional control experiments included incubation of sections in the absence of primary antisera or secondary antisera.

Comparison between ISH and IHC

A separate series of adjacent coronal sections (30 μm) was processed for GAD67 mRNA detection by ISH and GAD67 protein by IHC. IHC detection of GAD67 protein was performed similarly to methods described above. Adjacent sections were chosen as preliminary experiments with ISH for GAD67 mRNA followed by IHC detection of GAD67 protein demonstrated that the antigen (GAD67 protein) within the cell bodies does not survive the ISH procedure.

ISH

ISH detection of GAD67 mRNA was performed exactly as previously described (Weston et al., 2003). In brief, free-floating sections were placed into prehybridization mixture at room temperature for 30 minutes, then at 37°C for 1 hour. The riboprobes, prepared as described by Weston and colleagues (2003), were added directly to the prehybridization solution at a concentration of 50–100 pg/μl. After addition of the probe, the sections were placed at 55–60°C for 18–56 hours, then rinsed through decreasing concentrations of salt solutions, treated with a solution of RNAse A at 37°C, and also rinsed in the lowest salt concentration at 55°C for 30 minutes.

Sections were then processed for detection of the digoxigenin tag with a sheep polyclonal antidigoxigenin antibody conjugated to alkaline phosphatase (Roche, Indianapolis, IN). Sections were first incubated in a blocking solution of 10% horse serum for 30 minutes, then incubated in antidigoxigenin antibody (1:1,000) overnight at 4°C. After rinsing, the alkaline phosphatase was reacted with nitroblue tetrazolium (NBT) and 5-bromo-4-chloro-3-indolyl-phosphate,4-toluidine salt (BCIP) for 1–2 hours at room temperature under intermittent microscopic observation to determine optimal signal to noise (i.e., no signal in motor neurons, strong signal in known GABAergic areas). The reaction was quenched with 3 × 10-minute rinses in 0.1 M Tris/1 mM EDTA (pH 8.5). Sections were then rinsed and mounted on gel-coated slides, air dried, and covered with VectaShield (Vector) and coverslips attached with nail polish.

Immunoblot analysis for GAD

The immunoblot procedure was adapted from a previously published protocol (Foley et al., 2003). In brief, frozen cerebellar cortex samples obtained from three rats were solubilized in Laemmli buffer [62.5 mM Tris-Cl, pH 6.8, 2% sodium dodecyl sulfate (SDS), 160 mM dithiothreitol (DTT), 0.001% bromophenol blue, 6 M urea] and incubated for 30 minutes at 70°C. The samples (20 μl each) were loaded onto 4–12% acrylamide gradient SDS gel (NuPage Bris-Tris; Invitrogen, La Jolla, CA) and electrophoresed in 3-(*N*-morpholino)propane sulfonic acid (MOPS)-SDS buffer (50 mM MOPS, 50 mM Tris base, 3.4 mM SDS, 1 mM EDTA; Invitrogen). The proteins were transferred to polyvinvylidene difluoride membranes (Hybond-P; Amersham, Arlington Heights, IL) in 0.7 M glycine and 25 mM Tris base buffer. The membranes were blocked for 1 hour at room temperature in 5% skim milk powder in Tris-buffered saline-Tween 20 (TBS-Tween; 50 mM Tris base, 20 mM NaCl, 0.1% Tween 20) and incubated overnight in a primary antibody raised against either GAD67 (monoclonal mouse anti-GAD67; 1:5,000; MAB5406; Chemicon) or both GAD65/GAD67 (rabbit anti-GAD65/GAD67; 1:5,000; AB1511; Chemicon). The membrane was washed with TBS-Tween and incubated at room temperature for 1 hour in horseradish peroxidase (HRP)-conjugated sheep anti-mouse (1:2,000; Sigma) for the detection of GAD67 or goat anti-rabbit conjugated to HRP (1:2,000; Sigma) for the detection of GAD65 and GAD67. The membrane was again washed in TBS-Tween. Detection of the proteins was achieved by using enhanced chemiluminescence (ECL reagents; Amersham) and exposure to radiographic film (Hyperfilm ECL; Amersham).

Mapping of the localization of GAD67 immunoreactivity

Sections were examined under standard brightfield microscopy with a Zeiss AxioScope2 microscope. Regions of the medulla were determined with rat brainstem atlases (Paxinos and Watson, 1986; Paxinos et al., 1999).

Fig. 1. Characterization of antibody for GAD67. **A:** Immunoblot on rat cerebellar cortex from three rats (1–3). The left panel shows an immunoblot using the mouse monoclonal antibody raised against GAD67 (MAB5406; Chemicon), showing a distinct band at an approximate molecular weight of 67 kDa. The right panel shows the same samples incubated in a primary antibody raised against both GAD65 and GAD67, showing two distinct bands, one at approximately 65 kDa and one at 67 kDa. **B:** Photomicrograph of a section of rat brainstem incubated in the presence of both primary and secondary antibodies, demonstrating clear labeling in the dorsomedial medulla (see **inset**). **C:** Section adjacent to that shown in B, counterstained with neutral red. **D,E:** Control incubations in the absence of primary antibody raised against GAD67 or secondary antisera revealed a complete absence of nonspecific labeling throughout the medulla. Examination of sections incubated in the absence of either primary (D) or secondary (E) antisera showed no labeling in any regions of the medulla, even when viewed under higher magnification (see **insets**). 4V, fourth ventricle; AP, area postrema; DMV, dorsal motor nucleus of the vagus; Gr, gracile nucleus; NTS, nucleus tractus solitarius; sol, solitary tract; XII, hypoglossal nucleus. Scale bars = 50 μm.

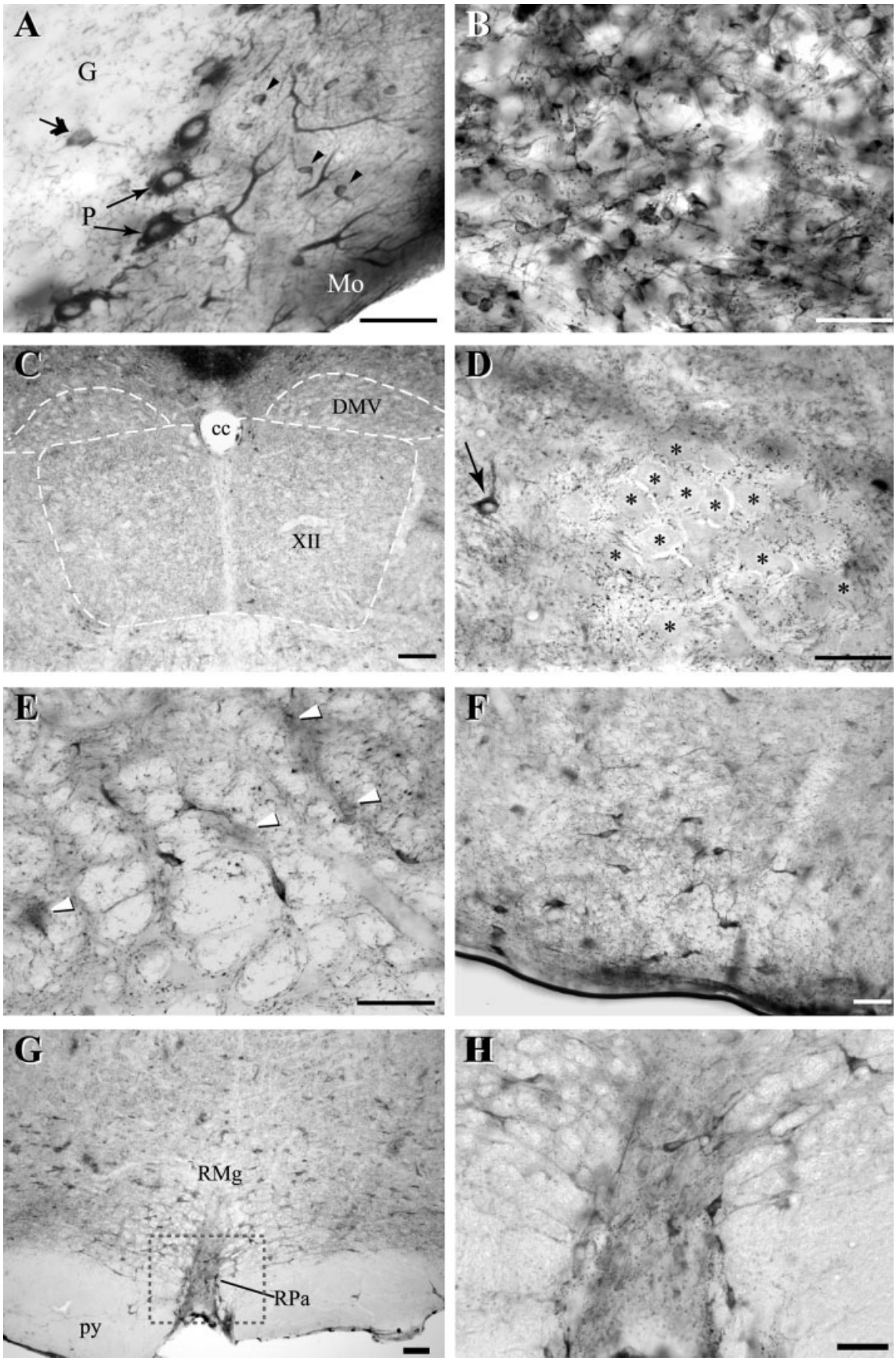

Figure 2

GAD67 immunoreactivity in the NTS

Sections 200 μm apart were used for the quantification of GAD67 immunoreactivity within the NTS. The sections were compared with an atlas of the rat brainstem (Paxinos and Watson, 1986; Paxinos et al., 1999) and divided into four rostrocaudal levels: NTS_{Ros}, NTS_{PV}, NTS_{subP}, and NTS_{cs}. NTS_{Ros} was defined as the level between the rostral pole of the hypoglossal nucleus and the level where the NTS is clearly adjacent to the floor of the fourth ventricle, approximately between bregma –12.42 mm and bregma –12.80 mm. NTS_{PV} was defined as the level where the NTS lies directly along the floor of the fourth ventricle, rostral to the rostral pole of area postrema, approximately between bregma –12.80 mm and bregma –13.54 mm. NTS_{subP} was defined as NTS at the level of area postrema, approximating bregma levels of –13.54 mm to –14.27 mm. NTS_{cs} was defined as the level caudal to area postrema from the level of calamus scriptorius, between bregma –14.27 mm and bregma –14.53 mm (Paxinos et al., 1999).

Subregions of the NTS were delineated by using the neutral red-stained section with reference to previous studies (Van Giersbergen et al., 1992) and atlases of the rat brainstem (Paxinos and Watson, 1986; Paxinos et al., 1999). Outlines of the subregions and major anatomical landmarks were delineated and drawn from the neutral red-counterstained section. This constructed map was then overlaid on the adjacent GAD67-ir section to identify subregion boundaries.

To determine the distribution of GAD67-ir cells in the NTS, the number of immunopositive neurons was examined in one-half of the brain throughout the four levels of the NTS described above, approximately from bregma –12.42 mm to bregma –14.3 mm, in a total of 53 sections from four rats, with each counted section separated by 200 μm. Cells were included only if the cell profile contained a complete cytoplasm and a clearly defined nucleus. The average number of cells per subregion on each section was scored as follows: 0–10 cells (+), 10–15 cells (++), 15–20 cells (+++), >20 cells (++++). For descriptive purposes, the terms sparse (+), moderate (++), high (+++), and dense (++++) will be used in the remainder of the text. The sampling method employed provides an estimate of the distribution of GAD67-ir cells within the NTS, because the total number of GAD67-ir cells cannot be provided without a full reconstruction of the NTS or the use of stereological methods (Coggeshall and Lekan, 1996; Saper, 1996). For descriptive purposes, in the remainder of the text, cell bodies <15 μm will be described as "small" cell bodies, whereas cell bodies >15 μm will be described as "large" cell bodies.

TABLE 1. Distribution of GAD67 Immunoreactivity within the Rat Nucleus Tractus Solitarius[1]

Region	No. of cells per hemisection	Varicosities
Commissural (Com)	+	+++
Subpostremal (subP)	+	+++
Gelatinous (Gel)	++	++
Dorsolateral (DL)	+	++
Interstitial (Int)	++	+++
Medial (Me)	++++	+++
Intermediate (IM)	+++	++
Central (Ce)	++++	+++
Lateral (Lat)	+	++
Ventrolateral (VL)	+	++
Ventral (V)	+	+
Parasolitary (PSol)	++++	++

[1]Number of cells is the average number of GAD67-positive cells in NTS subregions per hemisection. 0–10 cells (+), 10–15 cells (++), 15–20 cells (+++), >20 cells (++++; n = 4 rats). Density of varicosities was graded using a subjective scale: sparse (+), moderate (++), and dense (+++). Data represent the mean of observations made from (3 to 8) sections per subregion of the NTS in n = 4 rats.

The number of sections used to determine the density of GAD67-ir varicosities for each subregion varied between three and eight sections based on the rostrocaudal length of the subregion of interest. The following scale was used in grading the density of varicosities: 0 = absent; 1 = sparse, 2 = moderate, 3 = dense. The average score for each region was calculated and represented using the scale: sparse (+), moderate (++), high (+++).

Photomicroscopy, imaging, and camera lucida reconstruction

Sections were examined under standard brightfield microscopy with a Zeiss AxioScope2 microscope. Digital images were captured with a Nikon Insight digital camera and the imaging software Spot (version 4.0.8; Diagnostic Instruments, Sterling Heights, MI). The digital images were imported into Adobe Photoshop 6.0 (Adobe Systems, Mountain View, CA) and converted to gray scale.

Full section reconstructions by camera lucida drawing were performed on a representative section from each of the four defined levels of the NTS from one rat. Camera lucida drawings of GAD67-labeled neurons in the NTS were produced with a Zeiss microscope with a ×2.5 adjustable camera lucida drawing tube, under a total magnification of ×1,000. On average, each camera lucida drawing was reconstructed from nine fields of view (range = 6–12) at multiple focal planes (approximately five or six focal planes per field of view) to represent accurately the distribution of GAD67-ir cell bodies, fibers, and terminals throughout the 50-μm-thick section. The drawings were subsequently scanned in a flatbed scanner

Fig. 2. Brightfield photomicrographs of GAD67 immunoreactivity obtained from different levels of the rat medulla and cerebellum. **A:** GAD67-ir in the cell bodies and proximal processes of Purkinje cells (P, thin arrows), basket cells (arrowheads) in the molecular layer (Mo), and golgi cells (thick arrow) of the granular layer (G) of the cerebellum. **B:** Dense GAD67-ir cells, processes, and terminals in the area postrema. **C:** Lack of GAD67-ir cells in the hypoglossal nucleus (XII) and the dorsal motor nucleus of the vagus (DMV). **D:** GAD67-immunonegative cells (asterisks) located in the compact formation of nucleus ambiguus, surrounded by darkly stained terminals, whereas cells in the adjacent reticular field demonstrated GAD67-ir (arrow). **E:** GAD67-ir in the caudal ventrolateral medulla. Because of the thickness of the tissue, some GAD67-ir cells are out of focus (arrowheads). **F:** Large, intensely stained cells in the lateral paragigantocellularis, with the proximal processes of a number of cells clearly distinguishable. **G:** Large, scattered GAD67-ir cells can be distinguished in the raphe magnus (RMg), whereas the labeling in raphe pallidus (RPa) is much more concentrated. The adjacent pyramidal tract (py) shows sparse GAD67-ir. **H:** Magnified view of RPa from G. 4V, fourth ventricle; cc, central canal; DMV, dorsal motor nucleus of vagus; G, granular layer; Mo, molecular layer; P, Purkinje cell; py, pyramidal tract; RMg, raphe magnus; RPa, raphe pallidus; XII, hypoglossal nucleus. Scale bars = 50 μm.

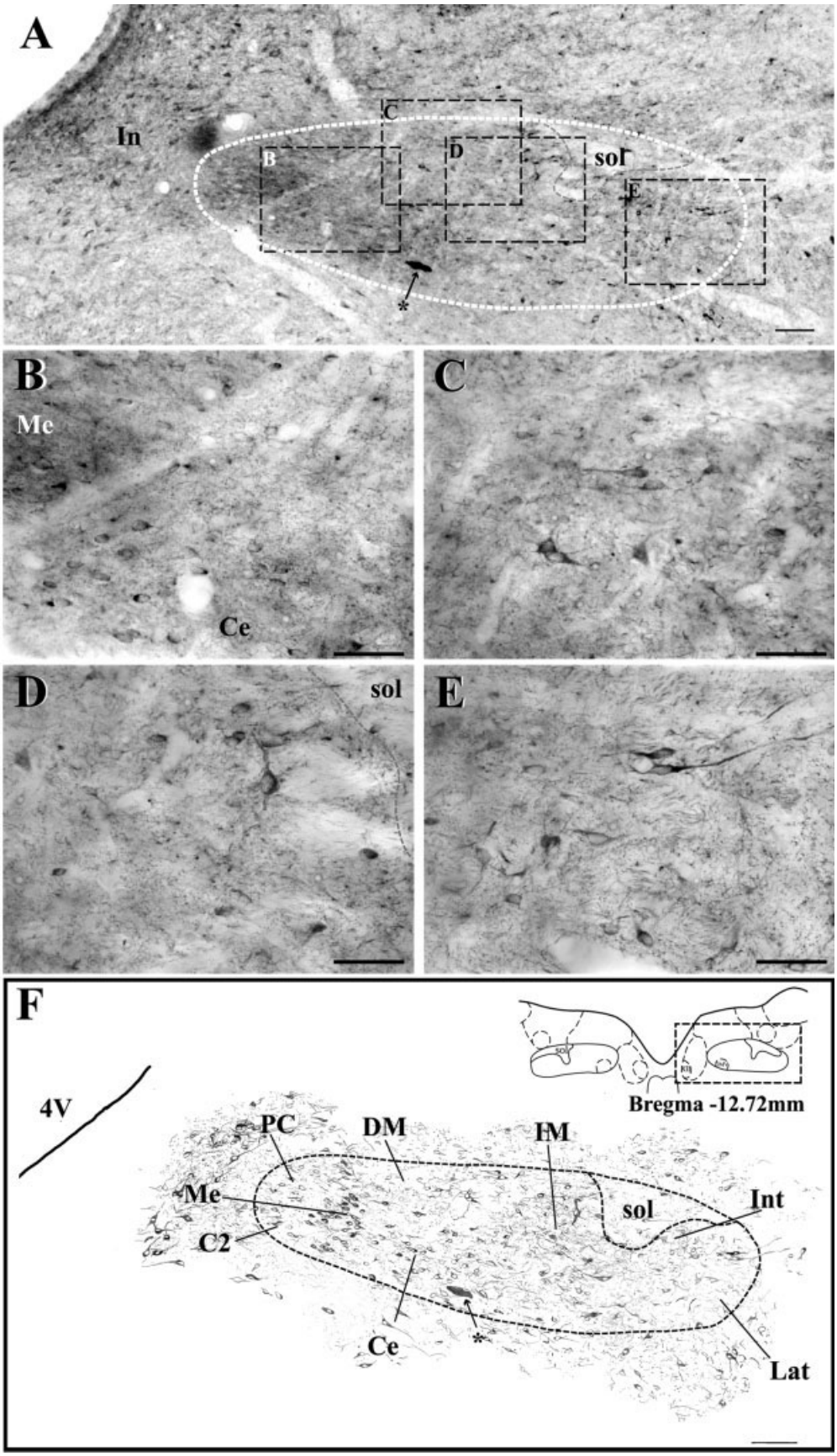
A
In
B
C
D
E
sol
*
B
Me
Ce
C
D
sol
E
F
4V
PC
DM
IM
Me
C2
sol
Int
Ce
*
Lat
Bregma -12.72mm

Figure 3

(Visioneer OneTouch 600) at a resolution of 600 dpi and assembled in Adobe Photoshop 6.0. All final figures were compiled with Adobe Illustrator 9.0 (Adobe Systems) and exported as gray-scale TIFF images at a resolution of 300 dpi.

RESULTS

Antibody specificity

The antibodies used in the current study were characterized as shown in Figure 1. An immunoblot of the mouse monoclonal antibody used in the current study (MAB5406) resulted in one distinct band at 67 kDa, whereas the rabbit polyclonal antibody (AB1511) clearly showed two distinct bands at approximately 65 kDa and 67 kDa in all three samples (Fig. 1A). Preliminary experiments on rat brain slices demonstrated reproducible immunoreactivity with minimal background at a concentration of 1/1,000 of the primary antibody in the absence of a permeabilizing agent such as Triton X-100 on vibratome cut sections (Fig. 1B). The introduction of Triton X-100 or cryosectioning resulted in a reduction of cell body labeling. Omission of either primary or secondary antibody resulted in a lack of reaction product (Fig. 1D,E).

General comment on GAD67 labeling

GAD67 immunoreactivity was visualized in cell bodies, fibers, and punctate structures (presumptive terminals) in most regions of the medulla. The reaction product was found in the neuronal cytoplasm surrounding the nucleus, but no nuclear staining was observed. The overall distribution of GAD67-ir cells in the medulla was similar to that previously described from ISH (Stornetta and Guyenet, 1999; Tanaka et al., 2003).

Regional distribution of GAD67 immunoreactivity in the medulla

In the cerebellum, the Purkinje cells (single arrows in Fig. 2A), basket cells (arrowheads in Fig. 2A), and Golgi cells (double arrow in Fig. 2A) were clearly labeled. GAD67-containing terminals were also found throughout granular layer and in fibers coursing through the cerebellar medulla. In the medulla, GAD67 immunoreactivity was visualized in cell bodies and punctate structures in most regions. GAD67-ir cell bodies, fibers, and punctuate structures were densely labeled in the area postrema (AP), typically as small, round or ovoid cells with complex arborizations (Fig. 2B). No GAD67-ir cells were localized in the dorsal motor nucleus of the vagus (DMV), the hypoglossal nucleus (XII; Fig. 2C), the nucleus ambiguus (NAmb.; see asterisks in Fig. 2D), or the facial nucleus, although GAD67-labeled terminals were clear. Immunoreactive cells, fibers, and terminals were also found in the caudal ventrolateral medulla (CVL; Fig. 2E), rostral ventrolateral medulla (RVL), and reticular fields (Fig. 2F). Large, darkly stained GAD67-ir cells, fibers, and terminals were seen consistently in the central cervical nucleus (CeCV) and the gracilus nucleus (Gr). In the external cuneate nucleus, fibers were predominantly labeled, with few GAD67-ir cells, whereas the cuneate nucleus (Cu) had sparse GAD67 labeling.

Intensely labeled GAD67-ir cell bodies, fibers, and terminals were found in the raphe nuclei, including raphe magnus (RMg; Fig. 2G), raphe pallidus (RPa; Fig. 2G,H), and raphe obscurus (ROb). The GAD67-positive cells in the RPa and ROb were mostly ovoid, whereas cells in the RMg were much larger. In the RPa, dense terminal labeling for GAD67-ir was also observed (Fig. 2H), and sparse, lightly labeled fibers were found in the adjacent pyramidal tract (py; Fig. 2H).

Other regions that contained GAD67-ir cells include the spinal trigeminal nucleus, paratrigeminal nucleus, medial nucleus of inferior olivary complex (IO), gigantocellular field dorsolateral to IO, prepositus nucleus (Pr), medial and spinal vestibular nuclei, and dorsal cochlear (DC) nucleus. Regions demonstrating dense immunoreactive terminals include the IO, DC, and Pr.

GAD67 distribution in NTS

GAD67-labeled cell bodies, fibers, and varicosities were expressed in all major subregions of the NTS (Table 1), the distribution of GAD67-ir in the NTS at the rostral, paraventricular, AP, and commissural levels is shown in Figures 3–6, respectively. In general, the level of GAD67 labeling of cells, fibers, and terminals was denser rostral to the calamus scriptorius. The majority of neurons in all subregions of the NTS that demonstrated GAD67-ir were small and round in appearance, whereas larger cells were consistently found in the lateral (Lat), ventrolateral (VL), and intermediate (IM) subregions.

GAD67 distribution in rostral NTS (NTS_{Ros}, bregma –12.42 mm to –12.80 mm)

All subregions of the NTS_{Ros} demonstrated GAD67-ir cells, fibers, and terminals. However, the distribution was heterogeneous among the different subregions at this level (Fig. 3). Fibers and dense terminals were found within the solitary tract, and large, darkly stained cells were also localized within the intersitial (Int) subregion. Medial to the solitary tract, the highest number of labeled cells was found in the medial (Me) and central (Ce) subregions (Table 1, Fig. 3B), where small, round immunoreactive cells were found in both regions, with a high density of terminal labeling. GAD67 expression in the intermedi-

Fig. 3. Photomicrographs (A–E) and representative camera lucida drawing (F) of GAD67-ir in the rostral NTS (NTS_{Ros}). **A:** Low-power photomicrograph montage of the NTS and surrounding regions showing the dense labeling of GAD67-ir in the medial and ventromedial aspects of the NTS. Solitary tract (sol) is outlined; asterisk indicates staining artifact. B–E: Photomicrographs taken at higher power of the boxed areas in A. **B:** Small, round somas were localized in the medial (Me) and central (Ce) subnuclei. **C,D:** Larger neurons were localized within the intermediate (IM) subregion. **E:** Large, darkly stained GAD67-ir cells were often localized within the lateral (Lat) subregion. **F:** Line drawing of section shown in A, demonstrating the heterogeneous distribution of GAD67 labeling throughout the NTS. Asterisk indicates the same artifact as in A. **Inset:** Corresponding section from a rat brain atlas (Paxinos and Watson, 1986). Nomenclature adapted from the atlas of Paxinos and colleague (1999). 4V, fourth ventricle; Ce, central subregion; DM, dorsomedial subregion; IM, intermediate subregion; In, intercalated nucleus; Int, interstitial subregion; Lat, lateral subregion; Me, medial subregion; PC, parvocellular subregion; sol, solitary tract. Scale bars = 100 μm in A,F; 50 μm in B–E.

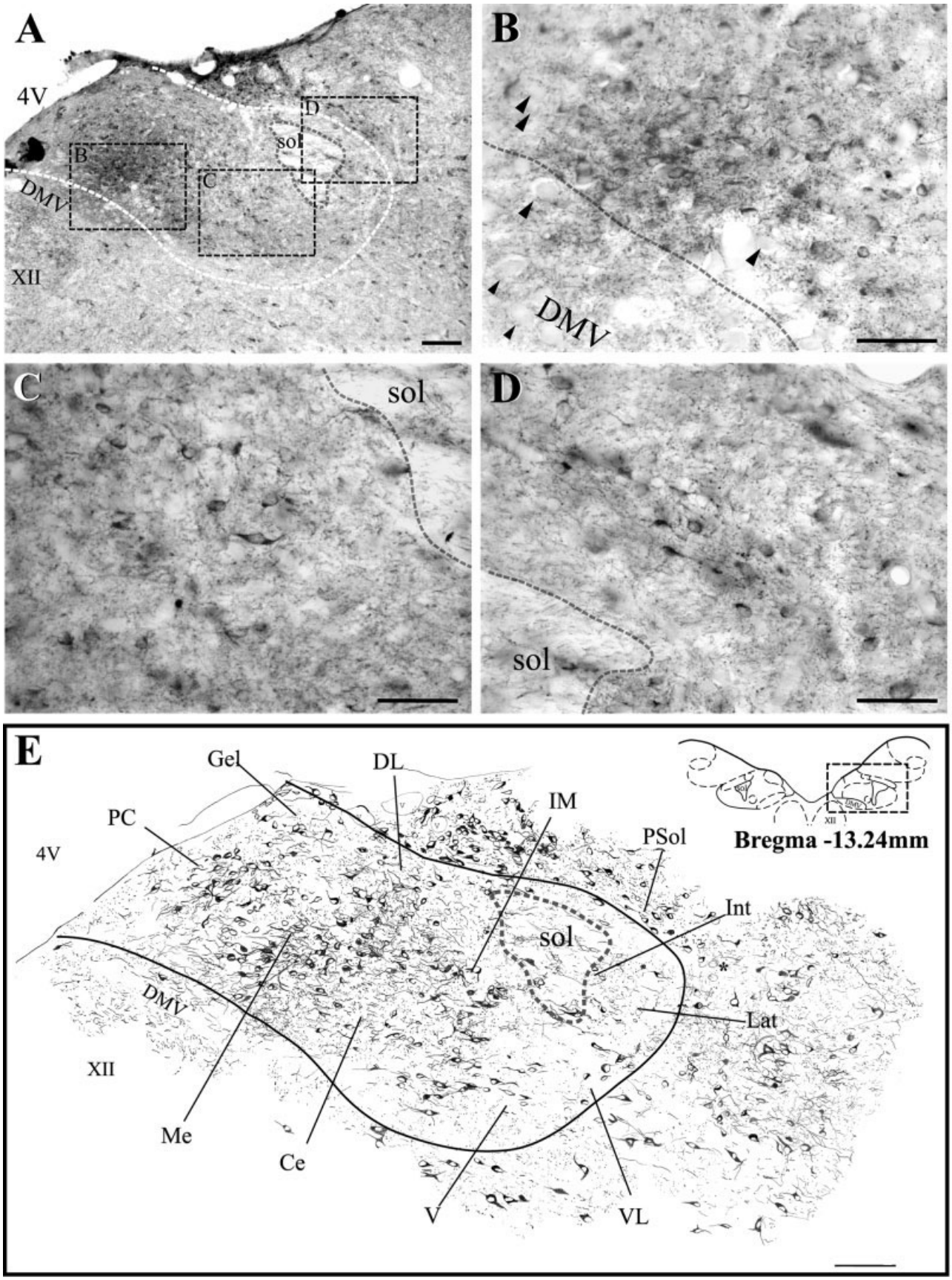
A
4V
B
C
D
sol
DMV
XII
B
DMV
C
sol
D
sol
E
Gel
DL
IM
PC
PSol
4V
Bregma -13.24mm
Int
sol
DMV
Lat
XII
Me
Ce
V
VL

Figure 4

ate (IM) subregion was present in small, round cells, similar to the adjacent Me and Ce subregions, but was also localized in larger cells (Fig. 3C,D), among a moderate density of terminals. Small, round immunoreactive cells were found in the dorsomedial (DM) and parvocellular subregion on the medial border of the NTS. A moderate density of GAD67-ir terminals and fewer cells were found within the lateral (Lat) subregion. On the lateral border of the NTS, some darkly stained cells with long processes were frequently observed (Fig. 3E). Figure 3F is a camera lucida reconstruction showing the location and density of GAD67-ir cells, fibers, and terminals throughout the thickness of this section from the rostral NTS.

GAD67 distribution in paraventricular NTS (NTS_{PV}, bregma –12.80 mm to –13.54 mm)

At the level of the fourth ventricle, large numbers of GAD67-ir cells were heterogeneously distributed throughout all the subregions (Fig. 4A). The greatest apparent density of GAD67-ir cells was found within the Me subregion, with a high density of GAD67-ir terminals (Fig. 4A,B, Table 1). Unlabelled cell bodies could be observed in the adjacent DMV and scattered between the densely labeled GAD67-ir cells in Me (arrowheads in Fig. 4B). Small, round immunoreactive cells were also found within the following subregions: Ce, parvocellular (PC), gelatinous (Gel), and dorsolateral (DL). In the IM subregion, larger, darkly stained cells were frequently observed in addition to small, round cells among a moderate density of GAD67-ir terminals (Fig. 4C, Table 1). Dorsal to the NTS, a high density of small round immunoreactive cells were found throughout the parasolitary subnucleus (PSol; Fig. 4D). In addition, a moderate density of GAD67-ir terminals was found throughout PSol. GAD67-ir fibers and terminals were found within the solitary tract (sol), with large, darkly stained cells within the Int subregion. Lateral to sol, moderate labeling of GAD67-expressing cells was found in the Lat, ventrolateral (VL) and ventral (V) subregions. In addition, moderate labeling of GAD67-ir terminals was observed in the Lat and VL, whereas only sparse labeling of GAD67 terminals was localized within the V subregion. Figure 4E is a camera lucida reconstruction showing the location and density of GAD67-ir cells, fibers, and terminals throughout the NTS_{PV}.

GAD67 distribution in subpostremal NTS (NTS_{subP}, bregma –13.54 mm to –14.27 mm)

In the midline, a moderate density of GAD67-ir cells and a high density of terminal labeling were observed in the commissural (Com) and subpostremal (subP) subregions (Fig. 5A,B, Table 1). Dense distribution of GAD67-ir cells, terminals, and fibers was found in the Me subregion at the level of the AP. GAD67-negative cell bodies could be found distributed within the Com, subP, and Me subregions as well as in the adjacent DMV (arrowheads in Fig. 5B). A high density of small, round GAD67-ir cells was found among GAD67-positive fibers and terminals in the Me and the adjacent Ce subregion (Fig. 5C). This is most clearly demonstrated in the camera lucida drawing in Figure 5E, demonstrating the tightly packed GAD67-ir cells, fibers, and terminals, in particular, in Me. In addition, larger, darkly stained cells were localized within the IM subregion, often with proximal processes clearly labeled (Fig. 5C). Dorsal to the NTS, the PSol subnucleus was again clearly distinguishable as a band of small, round GAD67-ir cells. Lateral to sol in the Int subregion, a dense distribution of GAD67-ir cells and terminals was found. In addition, short, darkly stained fibers were localized throughout this subregion, often obscuring the view of the GAD67-ir cells (Fig. 5D). In the Lat, VL, and V subregions, the GAD67-expressing cells were often larger than those in the other subregions at this level, including Me, Ce, subP, and Com. The GAD67-ir cells within the VL subregion were consistently more darkly labeled than the adjacent Lat and V subregions (see Fig. 5A,D). In addition, GAD67-ir terminal labeling in VL was more apparent and dense compared with the adjacent V and Lat subregions, with the lowest density of terminals found in the subregion V (Table 1). Figure 5E is a camera lucida reconstruction showing the location and density of GAD67-ir cells, fibers, and terminals in the subpostremal NTS.

GAD67 distribution in NTS at the level of calamus scriptorius (NTS_{CS}, bregma –14.27 mm to –14.53 mm)

Fewer GAD67-expressing cells were evident within the NTS at the level of calamus scriptorius compared with more rostral regions (Fig. 6A). In the Com and subP subregion, GAD67-ir cells could be observed, with dense GAD67-ir terminals apparent within both subregions. In the subP subregion, GAD67-ir cells with clear processes traversing horizontally through the section could be consistently visualized (Fig. 6B); this is best demonstrated in the camera lucida drawing (Fig. 6E). Lightly stained GAD67-ir cells, fibers, and terminals could be observed in the DL subregion, whereas the Me subregion could be clearly identified with darkly stained cells and dense terminal labeling (Fig. 6C). Lateral to the solitary tract (Fig. 6D), larger, darkly stained cells were also consistently observed. Figure 6E is a camera lucida reconstruction

Fig. 4. Photomicrographs (A–D) and camera lucida line drawing (E) of GAD67-ir in the NTS at the level of the fourth ventricle (NTS_{PV}). Photomicrograph taken at low magnification (**A**) of the NTS demonstrates greater GAD67 labeling in the NTS medial to the solitary tract (sol). The dorsal motor nucleus of vagus (DMV) and hypoglossal nucleus (XII) demonstrated no somatic label, whereas the parasolitary nucleus (PSol) showed high levels GAD67 labeling. Boxed areas in A are magnified in B–D. **B:** Magnified view of medial subregion (Me) showing GAD67 labeling of small, round cell, interspersed among dense terminal labeling. Arrowheads indicate unstained cells in the DMV and NTS. **C:** GAD67-ir cell bodies in the intermediate subregion (IM), medial to sol. **D:** Intense GAD67-ir in round cell bodies and terminals is apparent in PSol. **E:** Representative line drawing of GAD67-ir in section shown in A clearly shows the difference in the distribution of GAD67 labeling across the subregions. A schematic of the representative level from the rat brain atlas (Paxinos and Watson, 1986) is including in the **inset**. Nomenclature adapted from the atlas of Paxinos and colleague (1999). 4V, fourth ventricle; Ce, central subregion; DL, dorsolateral subregion; DMV, dorsal motor nucleus of the vagus; Gel, gelatinous subregion; IM, intermediate subregion; Int, interstitial subregion; Lat, lateral subregion; Me, medial subregion; PC, parvocellular subregion; PSol, parasolitary nucleus; sol, solitary tract; V, ventral subregion; VL, ventrolateral subregion; XII, hypoglossal nucleus. Scale bars = 100 μm in A,E; 50 μm in B–D.

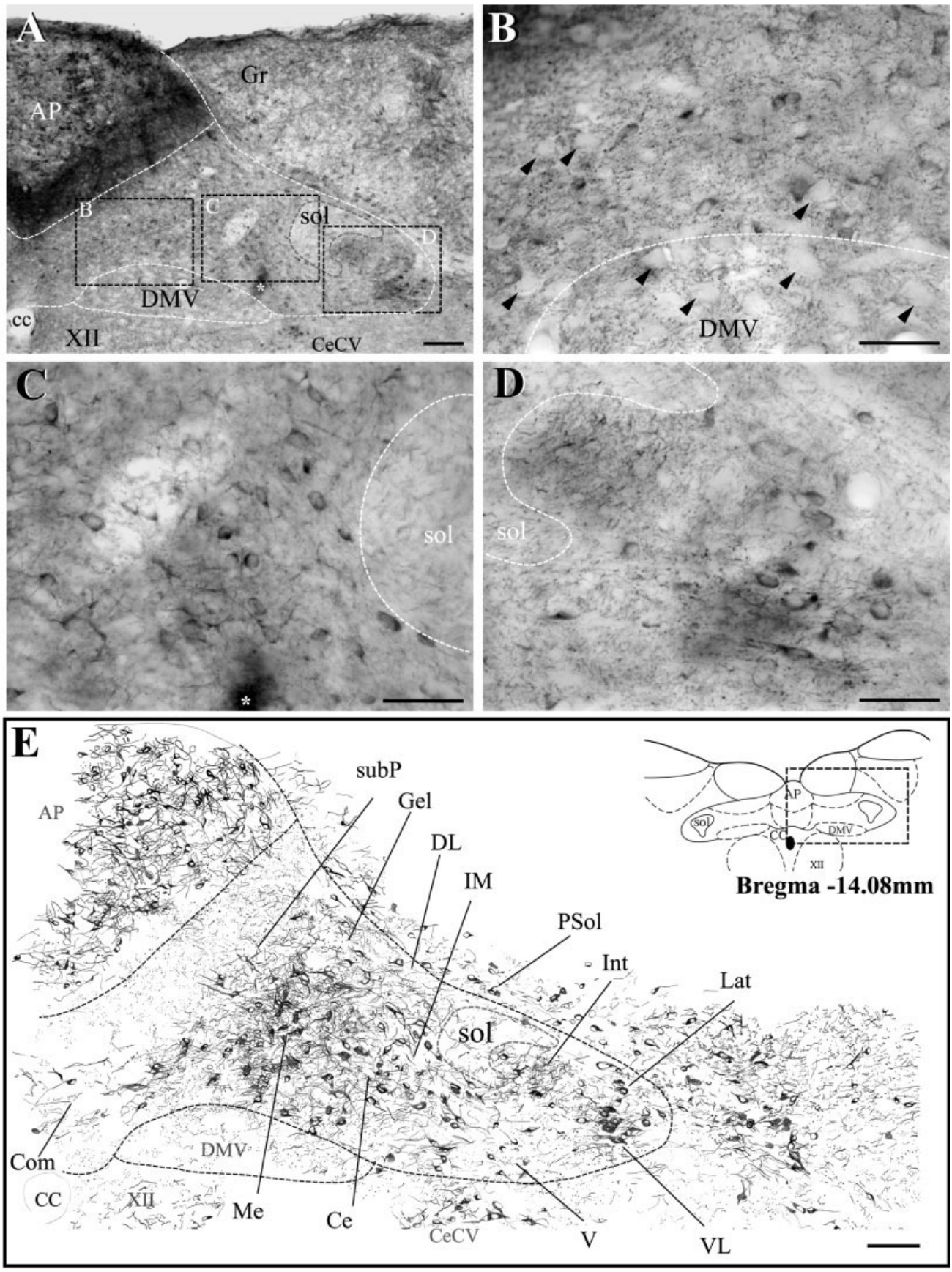
A
Gr
AP
B
C
sol
D
DMV
cc
XII
CeCV
B
DMV
C
sol
D
sol
E
subP
Gel
DL
IM
PSol
Int
Lat
AP
sol
DMV
Com
CC
XII
Me
Ce
CeCV
V
VL
Bregma -14.08mm

Figure 5

showing the location and density of GAD67-ir cells, fibers, and terminals in the NTS caudal to calamus scriporius.

Comparison between in situ hybridization for GAD67 mRNA and GAD67-ir

To demonstrate that our IHC method produced robust labeling of GAD67-expressing neurons, we used adjacent sections to compare our IHC procedure with a well-established ISH protocol (Stornetta and Guyenet, 1999). Results demonstrated strikingly similar distributions of GAD67-containing cells between both of these methods. Figure 7 illustrates two representative medullary regions, the NTS (Fig. 7A–D) and the midline raphe nucleus (Fig. 7E–H). In the NTS, the distribution and number of GAD67-labeled cells by IHC closely matched those shown by ISH performed in the immediately adjacent section. At higher magnification (Fig. 7C,D), GAD67-positive cells of the same approximate size were labeled by both methods. Although dense GABAergic terminal labeling in some NTS regions processed by IHC presented a challenge in identifying positively labeled cell bodies (see Fig. 7C), the overall patterns of labeling by both methods were similar. Similar results were also obtained in the raphe nucleus (Fig. 7E–H). Together, these results support the use of IHC to label and identify GAD67-expressing neurons in the rat medulla.

DISCUSSION

The current study provides the first detailed description of the distribution of GAD67 protein in the rat brainstem and, in particular, within the NTS. Our results demonstrate that GAD67 protein (both somatic and terminal labeling) was differentially distributed throughout the NTS, with the highest labeling density medial to the solitary tract. In addition, we found that the localization and distribution of GAD67-ir observed via standard IHC techniques were similar to the pattern of GAD67 mRNA observed via ISH. Our results suggest that detection of GABAergic neurons in the rat CNS is possible with standard IHC, without the toxic effect of colchicine.

General comments

In an earlier study by Esclapez and coworkers (1994), the distribution of GAD mRNAs and GAD proteins was similar throughout the forebrain and midbrain, suggesting that both IHC detection of GAD proteins and ISH detection of GAD mRNAs were reliable methods for the detection of GAD isoforms. Results from our IHC and ISH experiments are in agreement with results of Esclapez and colleagues and extend their observations by providing a semiquantitative assessment of the distribution of GAD67 cell bodies and terminals in the NTS.

For the medulla, previous studies have used ISH to localize GAD mRNA (Chan and Sawchenko, 1998; Stornetta and Guyenet, 1999; Tanaka et al., 2003). In particular, the study by Stornetta and Guyenet (1999) examined the distribution of the mRNA of both GAD isoforms (65 and 67) and found that both were present throughout the medulla. Although the levels of labeling between GAD65 and GAD67 were often different within the same region, there were no or very few regions that expressed one isoform exclusively. This suggests that both GAD65 and GAD67 may be good indicators of GABAergic neurons, although the individual roles of each GAD isoform are not well understood. To date, there has been no detailed description of the distribution of a specific GAD protein (either GAD65 or GAD67) within the medulla or the NTS using IHC methods. This has partially been due to the problem that the commercially available polyclonal antibodies provide predominantly terminal labeling (Liu et al., 2001, 2002). Moreover, these antibodies had limited success in labeling cell bodies without pretreatment with colchicine. However, the monoclonal antibody utilized in the present study, raised against GAD67, allows for the visualization of GAD67-expressing cell bodies without colchicine pretreatment.

GAD67-ir was detected in all brain regions that are known to contain GABAergic neurons, including the NTS, cerebellum, AP, RPa, RMg, ROb, and dorsal cochlear nuclei. In addition, all motor nuclei, including facial nucleus, NAmb, DMV, and hypoglossal nucleus, were devoid of GAD67-immunopositive cells. This is in agreement with previous studies (Chan and Sawchenko, 1998; Stornetta and Guyenet, 1999; Tanaka et al., 2003). Moreover, our control experiments using ISH and IHC on adjacent sections demonstrated that both methods detected a similar pattern of distribution of GAD67 mRNA and protein throughout the medulla. This provided additional verification of internal consistency between mRNA and protein labeling with these two methods.

Our experiments with double labeling for ISH followed by IHC on the same section demonstrated a lack of GAD67-ir cell bodies, although terminal labeling remained. Previous studies have demonstrated that it is possible to double label with ISH and IHC (Stornetta and Guyenet, 1999; Weston et al., 2003), suggesting that the antigen (GAD67 protein) in the cell bodies does not survive the ISH protocol. Although we cannot provide a definitive conclusion that the same population of neurons

Fig. 5. Brightfield photomicrographs (A–D) and camera lucida line drawings of GAD67-ir in the NTS at the level of area postrema (NTS_{subP}). **A:** Photomicrograph taken at low power demonstrating dense GAD67-ir in the AP and throughout the NTS. Boxed areas are magnified in B–D. Asterisk indicates staining artifact. **B:** Commissural subregion (Com) of the NTS and the adjacent dorsal motor nucleus of the vagus (DMV). Small, round cells and terminals are immunopositive for GAD67 in the Com, whereas no GAD67-ir cell bodies were localized in the DMV; arrowheads indicate unstained somas of the DMV and NTS. **C:** GAD67-ir cell bodies and a complex network of fibers can be discerned in the intermediate subregion (IM), medial to the solitary tract (sol). Asterisk indicates staining artifact. **D:** Large GAD67-ir cell bodies in the ventrolateral (VL) and interstitial (Int) subregions are clearly discernible. **E:** Representative line drawing of GAD67 distribution in the NTS and surround regions at the level of the AP. Dense GAD67-ir is found in the medial (Me), IM, Int, and VL subregions. Nomenclature adapted from the atlas of Paxinos and colleague (1999). AP, area postrema; cc, central canal; Ce, central subregion; CeCV, central cervical nucleus; Com, commissural subregion; DL, dorsolateral subregion; DMV, dorsal motor nucleus of the vagus; Gr, gracile nucleus; IM, intermediate subregion; Int, interstitial subregion; Lat, lateral subregion; Me, medial subregion; PSol, parasolitary nucleus; sol, solitary tract; subP, subpostremal subregion; V, ventral subregion; VL, ventrolateral subregion; XII, hypoglossal nucleus. Scale bars = 100 μm in A,E; 50 μm in B–D.

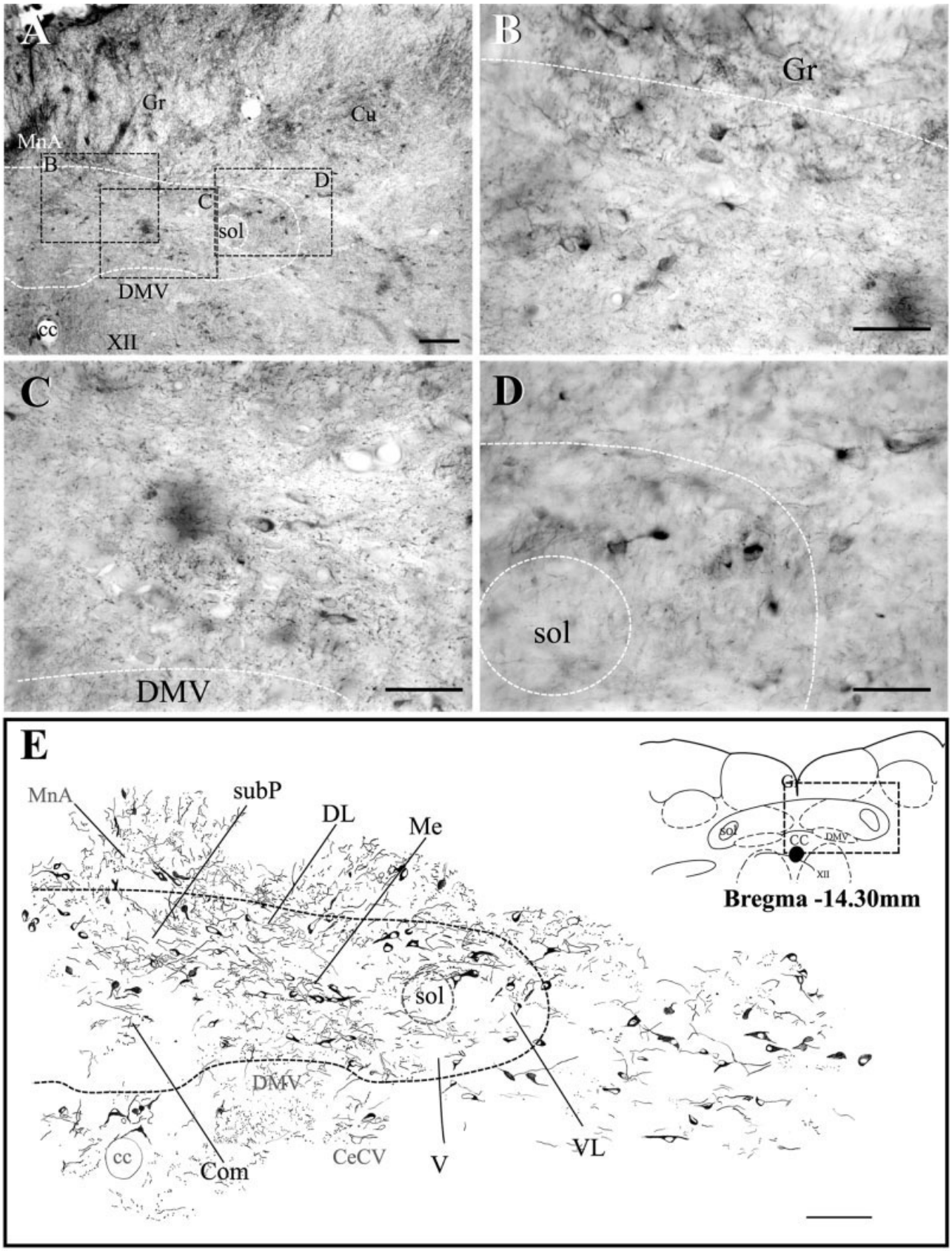
A
Gr
Cu
MnA
B
C
D
sol
DMV
cc
XII
B
Gr
C
DMV
D
sol
E
MnA
subP
DL
Me
sol
DMV
cc
Com
CeCV
V
VL
Gr
sol
CC
DMV
XII
Bregma -14.30mm

Figure 6

was visualized via IHC and ISH, similarities in the distribution pattern between our labeling and that in previous studies (Chan and Sawchenko, 1998; Stornetta and Guyenet, 1999; Tanaka et al., 2003) support the IHC detection of GAD67-expressing neurons with a monoclonal antibody.

Although a number of studies have examined the immunohistochemical distribution of GAD in the medulla (Blessing et al., 1984; Ruggiero et al., 1985; Meeley et al., 1985; Ellenberger, 1999), there were many caveats associated with the antibodies used in these earlier studies. One of the most limiting factors was the low level of labeling in cell bodies. To increase cell body labeling, the use of the microtubule-interfering agent colchicine was required to limit axonal protein transport (Blessing et al., 1984; Ellenberger, 1999). In the study by Blessing and colleagues (1984), it was clearly demonstrated that localization of GAD-positive neurons in the NTS was increased following colchicine pretreatment. However, the authors reported that, in the absence of colchicine, the distribution of GAD-ir cells was limited, and it did not reflect the GAD67 distribution demonstrated in later ISH studies (Stornetta and Guyenet, 1999; Tanaka et al., 2003). In addition, in these studies, the isoform of GAD against which the antibody was raised was unclear. This is of particular importance, insofar as recent evidence suggests that GAD65 and GAD67 might have differential intraneuronal distributions (Esclapez et al., 1994), so a nonisoform-specific antibody might preferentially identify terminals over cell bodies.

An additional benefit of IHC localization of GAD67 is the ability to visualize fibers and terminals, which is not possible with ISH. Although ISH reveals clear somatic labeling, this technique is limited to the localization of GAD67 mRNA-containing cell bodies. On the other hand, IHC reveals GAD67-ir terminals, fibers, and somas. GAD67, as detected by IHC, has been demonstrated as a reliable marker for GABAergic terminals (Murphy et al., 1998). Although the dense terminal label that we obtained by using this monoclonal antibody might hinder the observation of GAD-containing cells, the IHC detection of GAD67, with the present technique, has the benefit of allowing for the examination of both (presumptive) GABAergic terminals and cell bodies and the relationship between the two.

Distribution of GAD67 in NTS

In support of the data from the current study, the distributions of GAD67 mRNA in recent ISH studies (Chan and Sawchenko, 1998; Stornetta and Guyenet, 1999; Tanaka et al., 2003; Weston et al., 2003) and in our control experiments both demonstrated a similar pattern of labeling in the NTS. GAD67 mRNA-containing cells were found throughout all the rostrocaudal levels of the NTS, with a greater density of labeled cells rostral to calamus scriptorius and medial to the solitary tract, including dense labeling of GAD67 mRNA-containing cells in medial and interstitial subregions (Chan and Sawchenko, 1998). This is also consistent with an earlier biochemical study demonstrating greater GAD activity in rostral NTS compared with caudal regions, and higher GAD activity in medial NTS (Simon et al., 1985). This is in agreement with the current study, demonstrating a heterogeneous distribution of GAD67-ir in the NTS. In contrast, previous immunohistochemical studies reported a variable distribution of GAD- and GABA-containing cells in the NTS. The distribution of GABAergic cells ranged from a widespread distribution of GAD-ir in rat NTS (Blessing et al., 1984) and GABA-ir in cat NTS (Maley and Newton, 1985) to a low density of GAD-ir in rat NTS (Meeley et al., 1985; Miura et al., 1996) and GABA-ir restricted to the parvocellular region and immediately around the solitary tract in cats (Izzo et al., 1992). To complicate this problem further, the results varied based on whether colchicine was used. For example, the study by Blessing and colleagues (1984) found GAD-ir in VL and IM subregions in the absence of colchicine, whereas GAD-ir cells were localized in all subregions of the NTS following colchicine pretreatment. In other studies without colchicine pretreatment, GAD-ir cells were either totally absent (Ruggiero et al., 1985) or low throughout the NTS (Miura et al., 1996). These differences may be due to a number of factors, including the use of colchicine and placement of the colchicine injection. The current study is unique in that we used a monoclonal antibody raised against the specific isoform of GAD67, unlike previous immunohistochemical studies for GAD (Blessing et al., 1984; Meeley et al., 1985; Blessing, 1990). Furthermore, this antibody does not require pretreatment with colchicine to enhance somatic labeling, as was often required in the earlier immunohistochemical studies, and produced a similar distribution of GAD67-ir protein compared with GAD67 mRNA throughout the NTS.

Semiquantitative methods for examining GAD67-ir distribution in the present study revealed a subregional distribution of GAD67 within the rat NTS. The sampling method employed in our study provides strictly a representation, not the total number of GAD67-ir cells within the NTS (Coggeshall and Lekan, 1996). It was not possible to obtain a complete count of the total number of GAD67-containing neurons without first reconstructing the entire NTS or using stereological methods (Coggeshall and Lekan, 1996). The highest density of GAD67-ir in the present study was found in regions medial to the solitary tract,

Fig. 6. Brightfield photomicrographs (A–D) and camera lucida drawing of GAD67 distribution through the NTS at the level of calamus scriptorius (NTS_{CS}). **A:** Low-power photomicrograph of NTS, demonstrating GAD67-ir in the NTS and adjacent nuclei, including gracile (Gr), cuneate (Cu), and median accessory nucleus of the medulla (MnA). Cell bodies labeled for GAD67 can be seen in the NTS. Boxed areas are magnified in B–D. **B:** Higher magnification of GAD67 labeling in the dorsomedial NTS, on the border with Gr, in the subpostremal (subP) subregion. **C:** Medial (Me) subregion of the NTS, demonstrating somatic and terminal labeling for GAD67. **D:** Intense GAD67-ir in somas on the lateral edge of the NTS; note the lower level of terminal labeling compared with Me (C). **E:** Camera lucida drawing of the section photographed in A, demonstrating the difference in density of GAD67 labeling in the different subregions of the NTS. Nomenclature adapted from the atlas of Paxinos and colleague (1999). cc, Central canal; CeCV, central cervical nucleus; Com, commissural subregion; Cu, cuneate nucleus; DL, dorsolateral subregion; DMV, dorsal motor nucleus of the vagus; Gr, gracile nucleus; Me, medial subregion; MnA, median accessory nucleus; sol, solitary tract; subP, subpostremal subregion; V, ventral subregion; VL, ventrolateral subregion; XII, hypoglossal nucleus. Scale bars = 100 μm in A,E; 50 μm in B–D.

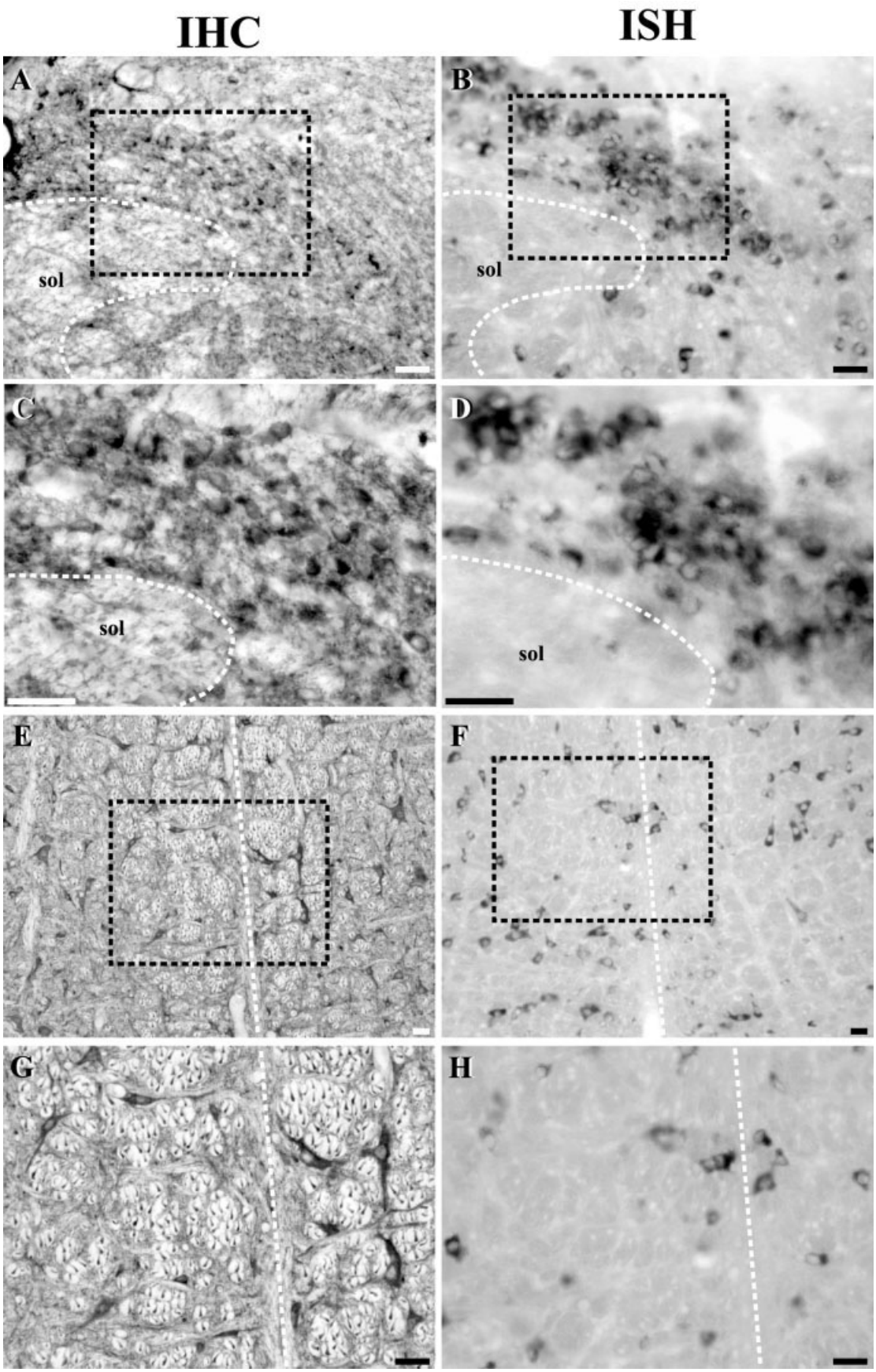

Fig. 7. Brightfield photomicrographs of adjacent sections processed for detection of GAD67 protein (A,C,E,G) and GAD67 mRNA (B,D,F,H) by immunohistochemistry (IHC) and in situ hybridization (ISH), respectively. Round cell bodies of similar size containing GAD67 protein (**A,C**) and mRNA (**B,D**) were localized in the nucleus tractus solitarius (NTS) lateral of the solitary tract (sol) and the parasolitary subregion dorsal of sol. Boxed areas in A and B are magnified in C and D, respectively. Numerous large GAD67-immunoreactive (**E,G**) cell bodies and GAD67 mRNA (**F,H**)-containing cells were localized in the midline medulla, in the region of raphe obscurus. Boxe areas in E and F are enlarged in G and H, respectively. Midline of the medulla is indicated by the white dashed line. Scale bars = 50 μm.

namely, the Me, IM, and Ce subregions, and in the parasolitary region. These regions receive a high density of arterial baroreceptor and chemoreceptor afferents (Ciriello, 1983; Finley and Katz, 1992; Ciriello et al., 1994) as well as somatosensory afferents from spinal dorsal horn (Craig, 1995; Gamboa-Esteves et al., 2001; Potts et al., 2003). In addition, the ventrolateral region of the NTS, which contained large, darkly stained GAD67-positive cells, has been demonstrated to receive pulmonary afferents (Cohen and Feldman, 1984). Together, these results suggest that the majority of NTS regions that receive sensory input from cardiovascular, somatosensory, and respiratory afferents contain a high density of GABAergic neurons. Because the NTS receives a wide range of peripheral sensory inputs, including gustatory, cardiopulmonary, and gastrointestinal (Kalia and Mesulam, 1980), it is likely that GABAergic neurons are involved in the modulation of these afferent inputs. The widespread distribution of GABAergic neurons within the NTS demonstrated in the present study supports the involvement of GABA in a host of different functions. However, because of the heterogeneous nature of the NTS, it may be difficult to interpret the functional relevance of the varied distribution within this nucleus at this time.

Several functional studies utilizing immunohistochemical detection of the early protooncogene protein product Fos to localize neuronal activation have identified a population of GABAergic neurons in the NTS activated by hypertension (Miura et al., 1996; Chan and Sawchenko, 1998; Weston et al., 2003). In particular, the study by Chan and Sawchenko (1998) reported that approximately 45% of neurons activated by hypertension were GABAergic. In addition, GABAergic interneurons in the NTS have been suggested to modulate the activity of second-order barosensitive neurons (Chen and Bonham, 2005). Although GABAergic neurons are involved in the processing of baroreceptor inputs to the NTS, only a small percentage of the total GABAergic population appears to participate in this reflex (Chan and Sawchenko, 1998). This suggests that the remaining GABA neurons likely modulate other incoming sensory signals. Indeed, neural input from both contraction-sensitive (Potts et al., 2003) and nociceptive (Boscan et al., 2002) somatic afferents has been shown to activate intrinsic GABAergic circuitry within the NTS that is independent of barosensory circuits. Processing of gustatory afferent input into the NTS also appears to involve GABAergic mechanisms (Bradley et al., 1996; Grabauskas and Bradley, 1996). Taken together, the findings from the current study support the notion that GABAergic neurons are an integral part of the intrinsic NTS circuitry (Kawai and Senba, 1996). Also, other studies have demonstrated inhibitory projections from the NTS (Aicher et al., 1995, 1996; Weston et al., 2003), including a GABAergic projection to the CVLM (Weston et al., 2003). Thus, it is likely that the GABAergic neurons labeled in the current study are involved in the modulation of inhibitory neurotransmission both intrinsic to the NTS and in other regions.

CONCLUSIONS

The present paper has described an alternative technique for the IHC visualization and localization of GAD67-containing neurons, as a marker for GABAergic neurons, in the rat brainstem, without the complication of colchicine use. This technique provides reproducible and consistent labeling of GAD67-expressing neurons, similar to that obtained from ISH. Furthermore, the present study provides the first systematic, detailed description of GAD67 labeling in the NTS, demonstrating a heterogeneous distribution of GABAergic neurons, fibers, and terminals. These results can aid in identifying the distribution of GABAergic neurotransmission within different subregions of the NTS.

ACKNOWLEDGMENTS

The authors thank Dr. Dennis Goebel for use of the camera lucida system and Dr. Anupam Gupta for assistance in tissue processing and analysis of GAD67 labeling.

LITERATURE CITED

Aicher SA, Kurucz OS, Reis DJ, Milner TA. 1995. Nucleus tractus solitarius efferent terminals synapse on neurons inthe caudal ventrolateral medulla that project to the rostral ventrolateral medulla. Brain Res 693:51–63.

Aicher SA, Saravay RH, Cravo S, Jeske I, Morrison SF, Reis DJ, Milner TA. 1996. Monosynaptic projections from the nucleus tractus solitarii to C1 adrenergic neurons in the rostral ventrolateral medulla: comparison with input from the caudal ventrolateral medulla. J Comp Neurol 373:62–75.

Blessing WW. 1990. Distribution of glutamate decarboxylase-containing neurons in rabbit medulla-oblongata with attention to intramedullary and spinal projections. Neuroscience 37:171–185.

Blessing WW, Ogawa H, Wang L. 1984. Glutamic acid decarboxylase immunoreactivity is present in perikarya of neurons in nucleus tractus solitarius of rat. Brain Res 322:346–350.

Boscan P, Kasparov S, Paton JF. 2002. Somatic nociception activates NK1 receptors in the nucleus tractus solitarii to attenuate the baroreceptor cardiac reflex. Eur J Neurosci 16:907–920.

Bradley RM, King MS, Wang L, Shu X. 1996. Neurotransmitter and neuromodulator activity in the gustatory zone of the nucleus tractus solitarius. Chem Sens 21:377–385.

Brambilla P, Perez J, Barale F, Schettini G, Soares JC. 2003. GABAergic dysfunction in mood disorders. Mol Psychiatry 8:721–737.

Chan RK, Sawchenko PE. 1998. Organization and transmitter specificity of medullary neurons activated by sustained hypertension: implications for understanding baroreceptor reflex circuitry. J Neurosci 18:371–387.

Chen C-Y, Bonham AC. 2005. Glutamate suppresses GABA release via presynaptic metabotropic glutamate receptors at baroreceptor neurones in rats. J Physiol 562:535–551.

Ciriello J. 1983. Brainstem projections of aortic baroreceptor afferent fibers in the rat. Neurosci Lett 36:37–42.

Ciriello J, Hochstenbach SL, Roder S. 1994. Central projections of baroreceptor and chemoreceptor afferent fibers in the rat. In: Barraco RA, editor. Nucleus of the solitary tract. Boca Raton, FL: CRC Press. p 35–50.

Coggeshall RE, Lekan HA. 1996. Methods for determining numbers of cells and synapses: a case for more uniform standards of review. J Comp Neurol 364:6–15.

Cohen MI, Feldman JL. 1984. Discharge properties of dorsal medullary inspiratory neurons: relation to pulmonary afferent and phrenic efferent discharge. J Neurophysiol 51:753–776.

Craig AD. 1995. Distribution of brainstem projections from lamina I neurons in the cat and monkey. J Comp Neurol 361:225–248.

Dampney RAL. 1994. Functional organization of central pathways regulating the cardiovascular system. Physiol Rev 38:323–364.

Dietrich WD, Lowry OH, Loewy AD. 1982. The distribution of glutamate, GABA and aspartate in the nuclues tractus solitarius of the cat. Brain Res 237:254–260.

Ellenberger HH. 1999. Distribution of bulbospinal gamma-aminobutyric acid-synthesizing neurons of the ventral respiratory group of the rat. J Comp Neurol 411:130–144.

Erlander MG, Tillakaratne NJK, Feldblum S, Patel N, Tobin AJ. 1991. Two genes encode distinct glutamate decarboxylases. Neuron 7:91–100.

Esclapez M, Tillakaratne NJ, Kaufman DL, Tobin AJ, Houser CR. 1994. Comparative localization of two forms of glutamic acid decarboxylase and their mRNAs in rat brain supports the concept of functional differences between the forms. J Neurosci 14:1834–1855.

Finley JCW, Katz DM. 1992. The central organization of carotid body afferent projections to the brainstem of the rat. Brain Res 572:108–116.

Foley CM, Stanton JJ, Price EM, Cunningham JT, Hasser EM, Heesch CM. 2003. $GABA_A$ α_1 and α_2 receptor subunit expression in rostral ventrolateral medulla in nonpregnant and pregnant rats. Brain Res 975:196–206.

Fong AY, Krstew EV, Barden J, Lawrence AJ. 2002. Immunoreactive localisation of $P2Y_1$ receptors within the rat and human nodose ganglia and rat brainstem: comparision with [α_{33}P]deoxyadenosine 5′-triphosphate autoradiography. Neuroscience 113:809–823.

Gamboa-Esteves FO, Tavares I, Almeida A, Batten TF, McWilliam PN, Lima D. 2001. Projection sites of superficial and deep spinal dorsal horn cells in the nucleus tractus solitarii of the rat. Brain Res 921:195–205.

Grabauskas G, Bradley RM. 1996. Synaptic interactions due to convergent input from gustatory afferent fibers in the rostral nucleus of the solitary tract. J Neurophysiol 76:2919–2927.

Izzo PN, Sykes RM, Spyer KM. 1992. γ-Aminobutyric acid immunoreactive structures in the nucleus tractus solitarius: a light and electron microscopic study. Brain Res 591:69–78.

Kalia M, Mesulam MM. 1980. Brainstem projection of sensory and motor components of the vagus complex in the cat: II. Laryngeal, tracheobronchial, pulmonary, cardiac, and gastrointestinal branches. J Comp Neurol 193:467–508.

Kawai Y, Senba E. 1996. Organization of excitatory and inhibitory local networks in the caudal nucleus of tractus solitarius of rats revealed in in vitro slice preparation. J Comp Neurol 373:309–321.

Kubo T, Kihara M. 1987. Evidence for the presence of GABAergic and glycine-like systems responsible for cardiovascular control in the nucleus tractus solitarii of the rat. Neurosci Lett 74:331–336.

Kubo T, Kihara M. 1988. Evidence for gamma-aminobutyric acid receptor-mediated modulation of the aortic baroreceptor reflex in the nucleus tractus solitarii of the rat. Neurosci Lett 89:156–160.

Kumada M, Terui N, Kuwaki T. 1990. Arterial baroreceptor refles: its central and peripheral neural mechanisms. Prog Neurobiol 35:331–361.

Kuwana S, Okada Y, Sugaware Y, Tsunekawa N, Obata K. 2003. Disturbance of neural respiratory control in neonatal mice lacking GABA synthesizing enzyme 67-kDa isoform of glutamic acid decarboxylase. Neuroscience 120:861–870.

Lawrence AJ, Jarrott B. 1996. Neurochemical modulation of cardiovascular control in the nucleus tractus solitarius. Prog Neurobiol 48:21–53.

Leonard NL, Renehan WE, Schweitzer L. 1999. Structure and function of gustatory neurons in the nucleus of the solitary tract. IV. The morphology and synaptology of GABA-immunoreactive terminals. Neuroscience 92:151–162.

Liu YY, Ju G, Wong-Riley MT. 2001. Distribution and colocalization of neurotransmitters and receptors in the pre-Botzinger complex of rats. J Appl Physiol 91:1387–1395.

Liu YY, Wong-Riley MT, Liu JP, Jia Y, Liu HL, Jiao XY, Ju G. 2002. GABAergic and glycinergic synapses onto neurokinin-1 receptor-immunoreactive neurons in the pre-Botzinger complex of rats: light and electron microscopic studies. Eur J Neurosci 16:1058–1066.

Maley B, Newton BW. 1985. Immunohistochemistry of γ-aminobutyric acid in the cat nucleus tractus solitarius. Brain Res 330:364–368.

Meeley MP, Ruggiero DA, Ishitsuka T, Reis DJ. 1985. Intrinsic gamma-aminobutyric acid neurons in the nucleus of the solitary tract and the rostral ventrolateral medulla of the rat—an immunocytochemical and biochemical study. Neurosci Lett 58:83–89.

Miura M, Okada J, Takayama K, Jingu H. 1996. Barosensitive and chemosensitive neurons in the rat medulla: a double labeling study with c-Fos/glutamate, GAD, PNMT and calbindin. J Auton Nerv Sys 61:17–25.

Murphy SM, Pilowsky PM, Llewellyn-Smith IJ. 1998. Pre-embedding staining for GAD67 versus postembedding staining for GABA as markers for central GABAergic terminals. J Histochem Cytochem 46:1261–1268.

Paxinos G, Watson C. 1986. The rat brain in stereotaxic coordinates. Sydney: Academic Press.

Paxinos G, Carrive P, Wang H, Wang P-Y. 1999. Chemoarchitectonic atlas of the rat brainstem. San Diego: Academic Press.

Potts JT, Paton JF, Mitchell JH, Garry MG, Kline G, Anguelov PT, Lee SM. 2003. Contraction-sensitive skeletal muscle afferents inhibit arterial baroreceptor signaling in the nucleus of the solitary tract: role of intrinsic GABA interneurons. Neuroscience 119:201–214.

Ruggiero DA, Meeley MP, Anwar M, Reis DJ. 1985. Newly identified GABAergic neurons in regions of the ventrolateral medulla which regulate blood pressure. Brain Res 339:171–177.

Saper CB. 1996. Any way you cut it: a new journal policy for the use of unbiased counting methods. J Comp Neurol 364:5.

Simon JR, DiMicco SK, Aprison MH. 1985. Neurochemical studies of the nucleus of the solitary tract, dorsal motor nucleus of the vagus and the hypoglossal nucleus in rat: topographical distribution of glutamate uptake, GABA uptake and glutamic acid decarboxylase activity. Brain Res Bull 14:49–53.

Stornetta RL, Guyenet PG. 1999. Distribution of glutamic acid decarboxylase mRNA-containing neurons in rat medulla projecting to thoracic spinal cord in relation to monoaminergic brainstem neurons. J Comp Neurol 407:367–380.

Sved AF, Sved JC. 1990. Endogenous GABA acts on $GABA_B$ receptors in nucleus tractus solitarius to increase blood pressure. Brain Res 526: 235–240.

Tabata M, Kurosawa H, Kikuchi Y, Hida W, Ogawa H, Okabe S, Tun Y, Hattori T, Shirato K. 2001. Role of GABA within the nucleus tractus solitarii in the hypoxic ventilatory decline of awake rats. Am J Physiol 281:R1411–R1419.

Tanaka I, Ezure K, Kondo M. 2003. Distribution of glycine transporter 2 mRNA-containing neurons in relation to glutamic acid decarboxylase mRNA-containing neurons in rat medulla. Neurosci Res 47:139–151.

Van Giersbergen PLM, Palkovits M, De Jong W. 1992. Involvement of neurotransmitters in the nucleus tractus solitarii in cardiovascular regulation. Physiol Rev 72:789–824.

Weston M, Wang H, Stornetta RL, Sevigny CP, Guyenet PG. 2003. Fos expression by glutamatergic neurons of the solitary tract nucleus after phenylephrine-induced hypertension in rats. J Comp Neurol 460:525–541.

Wong CG, Bottiglieri T, Snead OC III. 2003. GABA, gamma-hydroxybutyric acid, and neurological disease. Ann Neurol 54:S3–S12.